A Comparison of Switched Doubly-fed Machine Drive Topologies for High Power Applications

Arijit Banerjee, Steven B. Leeb, and James L. Kirtley
Department of Electrical Engineering and Computer Science, Massachusetts Institute of Technology
Cambridge, Massachusetts, USA
arijit@mit.edu, sbleeb@mit.edu, kirtley@mit.edu

***Abstract*—Doubly-fed machines (DFM) offer exciting possibilities for reducing power electronics requirements for variable speed drives (VSD). Design options are most versatile when the VSD DFM can be reconfigured "on-the-fly" in different winding and power connections. This paper presents a comparison of two different topologies of switched-DFM drives based on steady-state considerations. Effects of required drive torque, operating stator flux magnitude, and the machine parameters on the sizing of the rotor converter and on the drive performance for each of the topologies are analyzed and compared. The paper presents a holistic comparison of the two topologies to permit selection for particular application-specific requirements.**

***Index Terms*—Doubly-fed machine, propulsion drive, wide speed range, inverter sizing, power capability, high power, medium voltage drives.**

I. Introduction

Standard high power variable speed drives (VSD) show up as conveyors, pumps, fans, compressors, and also in propulsion applications for ships, locomotives, and off-highway vehicles [1]. In general, relatively high power VSDs use power converters rated at the shaft power, on the order of a few to several tens of megawatt. The converters control power flow to different electrical machine types depending on the drive, including permanent magnet [2], squirrel-cage induction [3], wound-rotor induction [4], and synchronous types [5]. Typically, component ratings and allowable switching frequency bound the design of the power electronics for a drive. For example, at present, the typical IGBTs used in medium voltage drives have voltage ratings of 3.3 kV, 4.5 kV or 6.5 kV that can switch at a few hundred Hz [6]. Multiple devices may be stacked together in series/parallel configurations to achieve high power capability. This has led to a considerable effort from research to product development focusing on different topologies for power-electronic building blocks (PEBB) to permit modular design with multilevel converters [7], [8], [9], [10].

A doubly-fed machine (DFM) can be exploited to reduce required power converter rating for a VSD. Of the four machine types typically available for high power applications, permanent magnet, squirrel-cage induction, and synchronous machines need a power converter of capability equal to that of the shaft power as these machines are inherently configured with a single electrical port and a single mechanical port for electromechanical energy conversion. However, the DFM has two accessible electrical ports to control energy conversion,

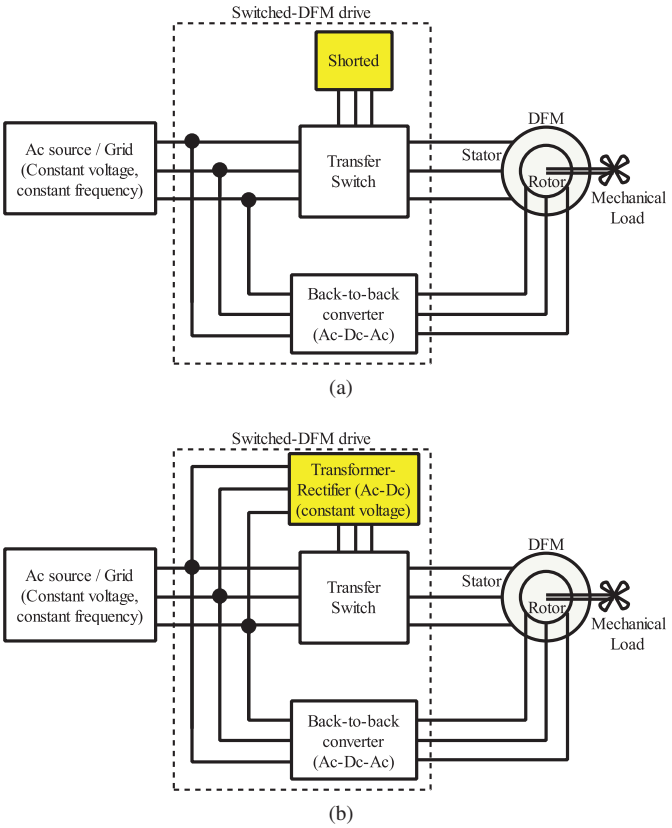

Figure 1. Reconfigurable architectures of switched doubly-fed machine drives (a) Low speed induction topology (LSI): At lower shaft speed, the stator is shorted (b) Low speed synchronous topology (LSS): At lower shaft speed, the stator is connected to a dc source. At higher shaft speed, the stator is connected to the ac source for both the topologies.

which adds a flexibility in the drive design considerations. This flexibility has been widely used in limited speed range applications, for example in wind power generation, to reduce the converter power rating to a third of the maximum shaft power [4]. For full speed range applications, including propulsion, the flexibility can be exploited with on-the-fly reconfiguration of the power connections to the DFM. Reconfigurable switched-DFM drives offer significant reduction of the operating fundamental frequency and on the power handled by the PEBB, typically to a third of the maximum shaft power, while allowing a full-speed range four-quadrant operation for

978-1-4799-7941-7/15/$31.00 ©2015 IEEE

the VSD [11]. In overview, the switched-DFM drives can have transfer switches that can connect one winding of the DFM to multiple sources or short them together while a controlled power converter controls electromechanical energy conversion from the other winding as shown in Fig. 1.

The different architectures of the switched-DFM drives reported in the literature can be broadly classified into two categories. In the first topology, named "Low-speed induction" (LSI), the DFM stator is shorted at lower drive speed [12], thereby emulating the DFM as a cage-induction machine as shown in Fig. 1(a). The rotor power converter provides both the complete shaft mechanical power and the total excitation current required by the DFM. In the second topology, termed "Low-speed synchronous" (LSS), the DFM stator is connected to a dc source at lower drive speed [13], thereby emulating the DFM as a wound-field synchronous machine. In this configuration, the rotor power converter provides the complete shaft power. The DFM magnetizing current is partly provided by the dc source and a constant stator flux is maintained using the rotor converter [14]. In either of the topologies, the DFM stator is connected to the ac source/grid at higher drive speed such that the rotor power converter controls the slip power to achieve a variable speed operation. The transition speed at which the DFM is reconfigured depends on the topology as well as on the required drive torque-speed characteristic. Usage of the thyristor-based transfer switches [15] instead of the mechanical switches [12], [13] and an appropriate control strategy on the controlled power converter [14] open up a huge opportunity to synthesize a high power drive with seamless drive performance. These drives have one-third rotor converter power rating, reduced filter requirements, improved machine-side and source-side harmonics, controllable power factor, and better drive efficiency which are all crucial components in the megawatt-level electromechanical energy conversion [8].

The LSI topology of the switched-DFM drive offers a significant reduction in the required components compared to the LSS topology that requires an additional dc source for low-speed operation. This paper compares the performance and requirements of the two topologies on the basis of the steady-state design considerations such as torque capability and utilization of the DFM, rotor power converter sizing, component count, transfer switch requirement, and structural noise. The comparison is useful from two different perspectives. First, the comparison can be used to select the topology that satisfies the drive requirement for a given DFM design. Second, the comparison can also be used to specify design guidelines for a DFM that suit the chosen topology for specific applications based on additional requirements.

II. Steady-state design and performance comparison

The well-known per-unit d-q model of a DFM in the stator-flux reference frame, as given in the Appendix, is used to illustrate the commonalities and the differences between the two topologies from the perspective of the steady-state operation. The parameters of a 1 HP, 220 V/ 150 V, 60 Hz, 4 Pole laboratory DFM, as given in Table. I, is used to compare the two topologies.

A. Torque capability

The torque capability of the DFM depends on the operating flux magnitude and the allowable currents in the stator and the rotor. As can be seen from (13), the torque producing q-axis currents in the stator i_{sq} and the rotor i_{rq} are directly proportional. However, the magnetizing d-axis currents in the stator i_{sd} and the rotor i_{rd} both contribute to the stator flux ψ_s at low-speed operation given by (12). The objective is to produce the desired drive torque τ in the DFM at low speed with the minimum stator flux magnitude and within the bounds of the allowable stator and the rotor winding currents. Minimizing the stator flux magnitude to achieve the required drive torque directly reduces the required rotor voltage, which impacts the drive size of the rotor converter [11].

An important parameter for the torque capability analysis is the designed rotor-to-stator current rating for the DFM I_r given by,

$$I_r = \frac{N\ I_{rms}|_{rotor}}{I_{rms}|_{stator}} \tag{1}$$

where N is the rotor-to-stator turns ratio and I_{rms} is the rms current rating of the winding. I_r governs the sharing of the magnetizing current of the DFM and is determined at the design stage of the machine. For a DFM designed for grid-connected motoring operation, the stator typically handles the magnetizing current completely, while the speed/torque control is achieved at the rotor-side [16]. Considering the stator current rating as the base current for normalization, the machine has I_r less than unity. Alternatively, for a DFM designed for the wind-power generation, the rotor is designed to provide the magnetizing current completely with higher margins for additional stator reactive power control [17]. The ratio I_r is greater than unity in such a machine.

For the LSI topology, the rotor d-axis current required to establish the stator flux ψ_s is given by,

$$i_{rd} = \frac{\psi_s}{x_m} \tag{2}$$

The torque that can be produced at the DFM shaft is simplified from (2) and (16) to get,

$$\tau = -\frac{x_m^2}{x_s} i_{rd} i_{rq} \tag{3}$$

However, the DFM must operate within the constraints of the allowable stator and the rotor currents. This can be formulated as:

$$\begin{aligned} i_{rd}^2 + i_{rq}^2 &\leq I_r^2 \\ i_{rq}^2 &\leq \left(\tfrac{x_s}{x_m}\right)^2 \end{aligned} \tag{4}$$

On the contrary, for the LSS topology, the stator flux is set by the stator current, while the d-axis rotor current is

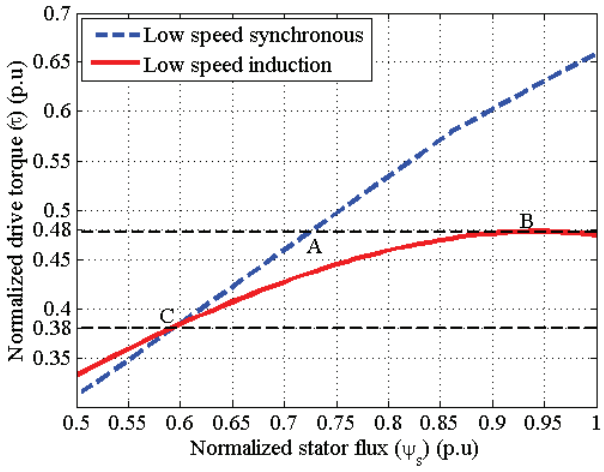

Figure 2. Comparison of the LSS and the LSI topology with respect to the torque capability at low speed operation for the example DFM.The LSS topology can extract more torque for a chosen stator flux magnitude for the example DFM compared to the LSI topology.

controlled to ensure a constant stator flux magnitude under different drive-torque demands. The torque that can be achieved from the DFM in this topology is given by [11],

$$\tau = \psi_s i_s \sin\delta \tag{5}$$

where i_s is the normalized stator current magnitude (dc) and δ represents the angle between the dc stator voltage and the stator flux vectors. Therefore, for a chosen stator flux magnitude ψ_s, the maximum torque that can be achieved from the DFM in the LSS topology is obtained by maximizing the product of the stator current magnitude and the sine of the angle δ subject to the following constraints below:

$$\begin{gathered} i_s \leq 1/\sqrt{2} \\ \left(-\tfrac{x_s}{x_m} i_s \sin\delta\right)^2 + \left(\tfrac{\psi_s}{x_m} - \tfrac{x_s}{x_m} i_s \cos\delta\right)^2 \leq I_r^2 \\ \left(-\tfrac{x_s}{x_m} i_s \sin\delta\right)^2 + \left(\tfrac{\psi_s}{x_m} - \tfrac{x_s}{x_m} i_s\right)^2 \leq I_r^2 \\ \delta < pi/2 \end{gathered} \tag{6}$$

The derivations of the constraints in (6) are detailed in [11]. The stator flux-torque characteristic achieved in the LSS topology using (5) and (6) is compared to the characteristic achieved in the LSI topology using (3) and (4) in Fig. 2 for the example DFM. The off-the-shelf example DFM is designed with I_r equals to 0.76. The LSS topology can extract higher torque from the machine compared to the LSI topology for a wide range of stator flux magnitude while remaining within the bounds of the stator and rotor current ratings. Therefore, for a desired drive torque it is more advantageous to use the example DFM in LSS topology as it allows for reduced operating stator flux magnitude. The reduction in operating stator flux magnitude directly translates into reduction in the required rotor converter voltage rating as will be shown in Section II-B.

However, the advantage on the torque capability for the individual topologies depend on the DFM design and more specifically on the I_r parameter defined in (1). The per-unit leakage and the magnetizing inductances of the example DFM are comparable to a typical DFM designed for multi-megawatt power rating [16]. The torque capabilities of the LSI and the LSS topologies are next evaluated using the same per-unit leakage and the magnetizing inductances of the example DFM, but as a function of I_r ranging from 0.75 to 1.25. The range corresponds to the borderline cases when the magnetizing current for the DFM is provided either completely by the stator or by the rotor windings. This range includes typical magnetizing current requirement of 10% - 30% of rated current for a high power DFM [16]. The torque capability of the DFM in the LSI and the LSS topologies vary with the design parameter I_r for a particular stator flux magnitude as shown in Fig. 3. The comparison implies that more drive torque per stator flux can be achieved using the LSI topology for a DFM designed to handle the magnetizing current from the rotor. Conversely, the LSS topology is preferable for a DFM designed to handle the magnetizing current from the stator.

However, the parameter I_r also influences drive-end converter current rating as the converter has to be additionally rated for the magnetizing currents of the DFM. Therefore, for an open design, a trade-off between the rotor converter voltage rating, current rating, and the design of the DFM based on the desired drive torque and sharing of the magnetizing current between the stator and the rotor dictates the choice of the preferable switched-DFM topology.

B. Rotor-side power converter rating

The rating of the rotor-side power converter depends on the voltage, current, and the maximum fundamental frequency rating required for the drive to operate over the full-speed

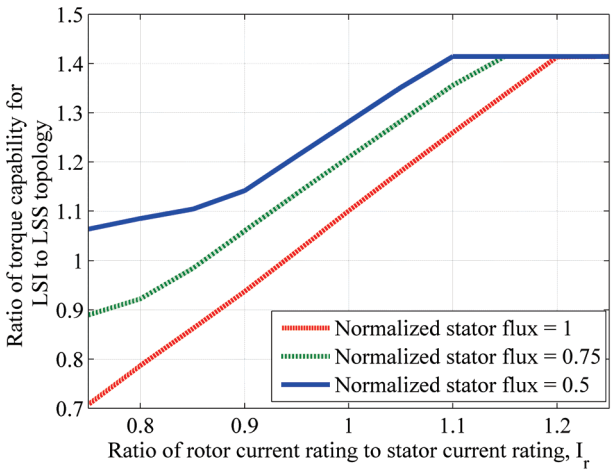

Figure 3. Effect of the stator and the rotor winding current ratings on the torque capability of the DFM during low speed operation. The LSI topology is preferable over the LSS topology for the DFM designed with a higher rotor current rating.

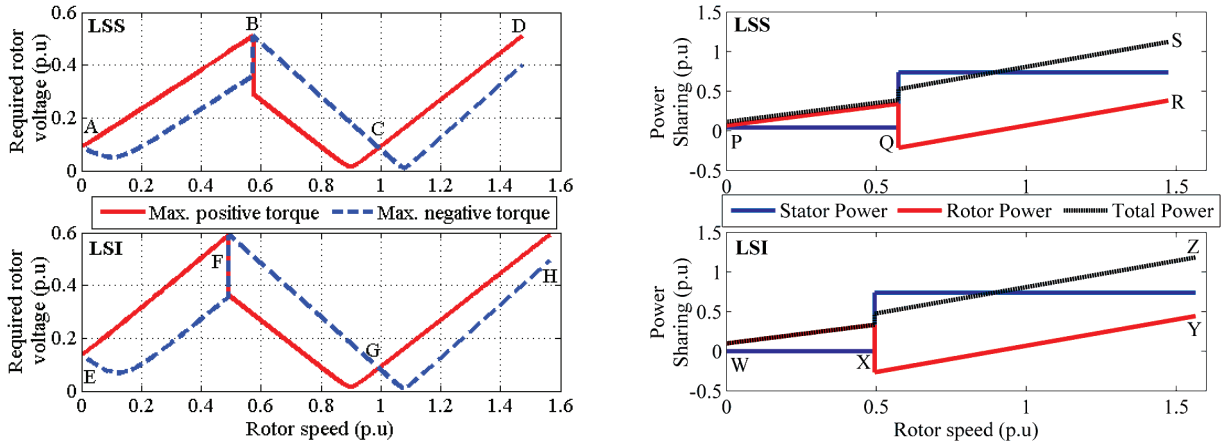

(a) (b)

Figure 4. Comparison of the LSI and the LSS topologies based on (a) the required rotor converter voltage rating and, (b) active power sharing between the stator and the rotor for the example DFM.

range. The current rating is governed by the drive torque requirement and by the DFM design for sharing of the magnetizing current. For proper utilization of the DFM, the current rating of the rotor converter is predominantly set by the required rotor current to achieve the rated torque at full-speed operation with the stator connected to the ac-source. Therefore, the rotor converter current rating does not depend on the topology of the switched-DFM drive. However, the voltage rating is dependent on the low-speed mode operation and, therefore, depends on the choice of topology. Two case studies using different drive torque requirements at low-speed for the example DFM highlight the impact of the choice of stator flux magnitude and DFM parameters on the required rotor converter voltage rating for the individual topologies.

1) Identical drive torque achieved at different stator flux magnitude: For example, assuming the required drive torque at low speed corresponds to 0.48 p.u (72% of the high-speed torque capability of 0.66 p.u) for the example DFM implies that the required operating stator flux has to be 0.94 p.u in the LSI topology and 0.725 p.u in the LSS topology. This corresponds to the operating points A and B respectively in Fig. 2. Based on the chosen operating stator flux magnitude, the required rotor voltage for the operation of the DFM in the individual topologies for the maximum positive and negative drive torque is calculated using (8)-(15) and is shown in Fig. 4(a). Not surprisingly, the required rotor voltage is identical in the high-speed ac-source-connected operation of the DFM for both the topologies. This corresponds to the segments BCD and FGH. However, the higher operating stator flux in the LSI topology increases the slope of the required rotor voltage versus rotor speed curve at low-speed operation (corresponding to the segment AB and EF). This results in a 16% increase in the required rotor voltage for the LSI topology compared to the LSS topology. The transition speed for low-speed to high-speed configuration is adjusted to minimize the required rotor voltage for operation across the complete speed-torque range [11]. An increase in rotor voltage margin also influences the maximum operating speed range in the high-speed grid-connected mode. In the example DFM, the maximum speed that can be achieved by the LSI topology is 6% higher compared to that of LSS topology for the same ac source synchronous speed.

The active power sharing between the stator and the rotor of the DFM at the maximum positive drive torque for the two topologies is compared in Fig. 4(b). In the low-speed operating regime in the LSS configuration, the stator supplies the resistive losses in the stator winding. This is represented by non-zero segment of PQ. The maximum active power handled by the rotor converter is 34% of the maximum total active power delivered to the DFM in the LSS configuration for the example DFM (corresponding to the operating points R and S in Fig. 4(b)). During low-speed operation in the LSI topology, all the active power to the DFM is supplied through the rotor including the stator resistive losses. The maximum active power handled by the rotor converter is 38% of the maximum total active power delivered to the DFM, corresponding to the operating points Y and Z respectively in Fig. 4(b).

2) Identical drive torque achieved at identical stator flux magnitude: The next case study illustrates the effect of the DFM parameters on the required rotor voltage operating with an identical stator flux magnitude. For example, a drive torque requirement of 0.38 p.u (58% of the high-speed mode torque capability) for the example DFM during low-speed operation results in identical stator flux requirement in both the topologies as can be seen in Fig. 2 by operation point C. The goal is to investigate whether the DFM parameters (excluding resistance) have any significance on the choice of topology based on the required rotor voltage under identical stator flux operation. Assuming negligible resistances, the required rotor voltage magnitude can be written using (8) - (16) as,

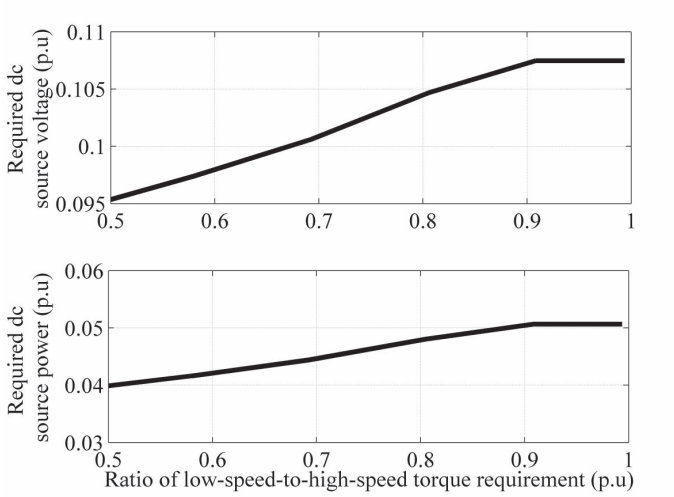

Figure 5. Requirement of the dc source for the low speed operation in LSS topology for different drive torque requirement (a) required voltage level (b) required power rating for the example DFM.

$$v_r = (\omega_s - \omega_e)\sqrt{\underbrace{\left(\sigma\frac{\tau}{\psi_s}\right)^2}_{d} + \underbrace{\left(\frac{x_r\psi_s}{x_m} - \sigma i_{sd}\right)^2}_{q}} \quad (7)$$

where $\sigma = \left(\frac{x_r x_s - x_m^2}{x_m}\right)$. Under same drive torque requirement and stator flux magnitude, the d-axis component of the required rotor voltage is independent of the topology. The q-axis component of the rotor voltage is dependent on the d-axis stator current. For the LSI topology, i_{sd} is inherently zero by configuration. For the LSS topology, i_{sd} $(= i_s \cos\delta)$ tends towards zero at the maximum drive torque as the angle δ approaches $90°$. The operating condition at full drive torque implies that the stator current vector is nearly orthogonal to the stator flux vector and the stator flux magnitude is completely supported by the d-axis rotor current. Therefore, the q-axis rotor voltage is not significantly different in either of the LSS or the LSI topologies at an identical drive torque and stator flux conditions. At steady state, the stator flux frequency ω_s is zero in the LSS topology. In the LSI topology, ω_s corresponds to the slip frequency, which tends to be very small for high power machines. Hence, for negligible resistances, the required rotor voltage is independent of the choice of topology for a given DFM.

In conclusion, the required rotor voltage is dependent predominantly on the choice of the stator flux magnitude to achieve the desired drive torque at low-speed operation. The preferable topology in this regard greatly depends on the topology that allows one to achieve the desired torque at minimum stator flux, which indirectly depends on the DFM design for magnetizing current sharing between the stator and the rotor.

C. Requirement of a separate dc source

The absence of a separate dc source makes the LSI topology attractive due to reduced component counts and complexity of additional source requirement. The dc source needed for the LSS topology can be made using a transformer-diode bridge rectifier. Typically, a transformer is connected between the rotor side converter and the grid. An auxiliary winding on this transformer may be used to supply a three phase bridge rectifier to create the dc source. The dc source power rating depends on the stator copper losses, which are typically a fraction of the rated drive power. For the example DFM with stator resistance of 0.1 p.u, the required dc source voltage is ~ 0.1 p.u and the power rating is of the order of 0.045 p.u for the different low-speed-to-high-speed drive torque design requirement as shown in Fig. 5. The p.u resistance of a high-power DFM is in the order of $0.01 - 0.02$ p.u. This calls for an even smaller dc source with a lower voltage and power rating requirement. The required power rating of the dc source is similar to the additional power rating required by the LSI topology compared to the LSS topology.

D. SCR-ratings for the Transfer Switch

The thyristor-based transfer switch for the LSS topology [15] can be adopted for the LSI topology, as shown in Fig. 6. The six silicon controlled rectifiers (SCRs) connected between the ac source and the stator of the DFM behave identically irrespective of the low-speed topology. In the LSI topology, six of the SCRs $T^A_{dc,F}$, $T^A_{dc,R}$, $T^B_{dc,F}$, $T^B_{dc,R}$, $T^C_{dc,F}$, and $T^C_{dc,R}$ that short the stator carry half cycle slip-frequency stator current and, therefore, need to be rated with identical current carrying capability. In the LSS topology, the SCRs $T^A_{dc,F}$, $T^B_{dc,R}$, and $T^C_{dc,R}$ carry the dc current to the stator winding under steady-state operation. The complementary SCRs on the dc source side, $T^A_{dc,R}$, $T^B_{dc,F}$, and $T^C_{dc,F}$ provide a path for the stator current only during the transients and high-speed-to-low-speed source transition operation. Therefore, these complementary SCRs can be selected based on the transient current requirement.

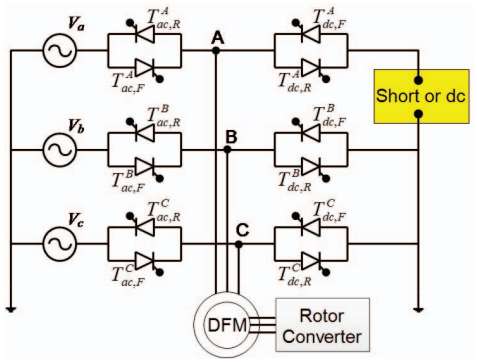

Figure 6. SCR-based transfer switch can be easily adopted for either of the two topologies for seamless mode transition.

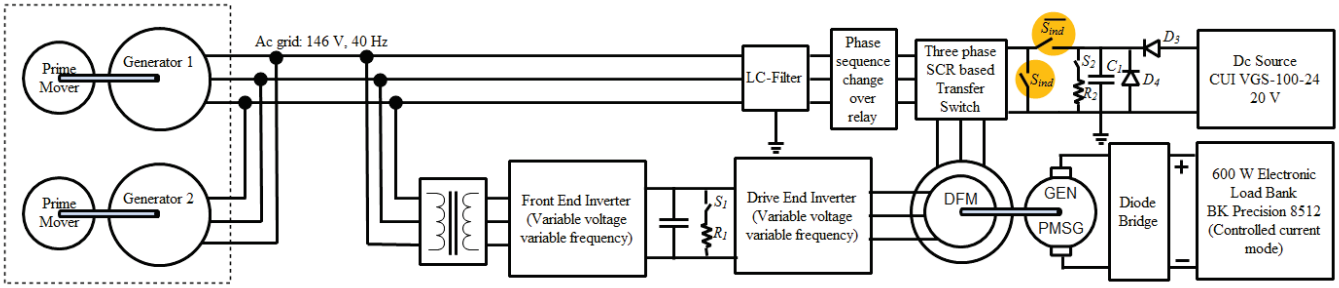

Figure 7. Experimental setup used to compare the two topologies of the switched-DFM drive. The ac source/grid voltage and frequency levels are chosen such that the example DFM operates within the rated speed and at rated stator flux condition.

E. Structural vibration and noise

Structural vibration and noise in an electrical machine may arise due to mechanical forces, electromagnetic forces, and aerodynamic forces [18]. The most important source of structural vibration is the electromagnetic force that arise due to the time-varying magnetic fields. Magnetic flux densities in the stator and the rotor interact with each other to produce magnetic stress waves. The magnitude of the stress wave is proportional to the amplitude of the flux densities and acts in the radial direction on the stator and rotor active surfaces. The radial force produce deformations in the magnetic circuit both in the rotor and the stator structures. The stator frame forms the primary source of the machine noise as it is typically connected to a mounting platform, which can act as a transmitting medium. Additional inconsistencies in the magnetic path due to the effect of slotting, winding distribution, rotor eccentricity, magnetic saturation, and saliency add on to the variation in radial magnetic force for generation of the noise and vibration in the machine.

The switched-DFM drive in LSS topology produces a stationary magnetic field in the stator and the rotor. Although the radial force does exist, the lack of the time-varying feature of the force on the stator ensures static deformation of the stator structure. This implies that the LSS topology is beneficial in applications as in naval propulsion, where low structural noise is of prime importance during low-speed stealthy maneuvers. The switched-DFM drive in the LSI topology produces a stator magnetic field that rotates at the slip frequency. The low frequency time varying magnetic field produces different modes of magnetic stress waves that form the source of vibration and noise for the electrical machine. As low frequency sound can travel very far underwater, the LSI topology can result in higher levels of detectability when used in naval applications [19]. Additional consideration during the mechanical design of the DFM must be taken into account to ensure that these modes do not overlap with the mechanical resonant frequencies of the stator structure. Proper structural mounting and damping can reduce the propagation of the noise through the stator structure, and can be easily adopted for any civilian applications.

III. Experimental Results

Experiments have been performed on the example DFM to compare the performance of the LSS and the LSI topologies of the switched-DFM drive while the DFM is operated within the rated condition. The laboratory setup comprises an ac grid of 146 V (line-to-line, rms), 40 Hz that is made from two synchronous generators operating in parallel as shown in Fig. 7. The choice of the ac grid frequency ensures that the off-the-shelf example DFM remains within the rated operating speed of 1800 rpm even when running at super-synchronous speed. Correspondingly, the ac source voltage magnitude is adjusted to ensure a rated stator flux operation of the DFM in the grid-connected mode. The rotor of the DFM is connected to the back-to-back converters that can produce variable voltage variable frequency ac waveforms at the rotor terminal from the fixed frequency ac grid. The converters are made from two Texas Instruments High Voltage Motor Control & PFC Developer's Kits connected in a back-to-back configuration. The controller is programmed in TMS320F28035 placed in these Kits. A SCR-based transfer switch enables on-the-fly connection of the stator of the DFM either to the grid or to the low speed operating topology. Two complementary switches S_{ind} and $\overline{S}_{ind}$ are used to preselect the topology for the experiment. Turning ON the switch S_{ind} makes the DFM operate in the LSI topology while turning the switch OFF configures the DFM to operate in LSS topology with the stator being connected to a separate 20 V dc source during low speed operation. The control architecture and the SCR-based transfer switch operating algorithm is modified depending on the topology. The DFM is mechanically loaded by a permanent magnet synchronous generator (PMSG) coupled with a dc electronic load bank. The load bank emulates different load torque variation at the shaft including the typical quadratic load torque profile in a ship propulsion.

The switched DFM drive is designed to achieve identical drive torque capability for both the topologies. The drive is designed with a low-speed torque capability of 70% of the high-speed torque capability. The LSI topology operates with a stator flux of 0.36 V-s at low speed and the LSS topology operates with a stator flux magnitude of 0.32 V-s at low speed to achieve the same drive torque. The mode-transition speed is

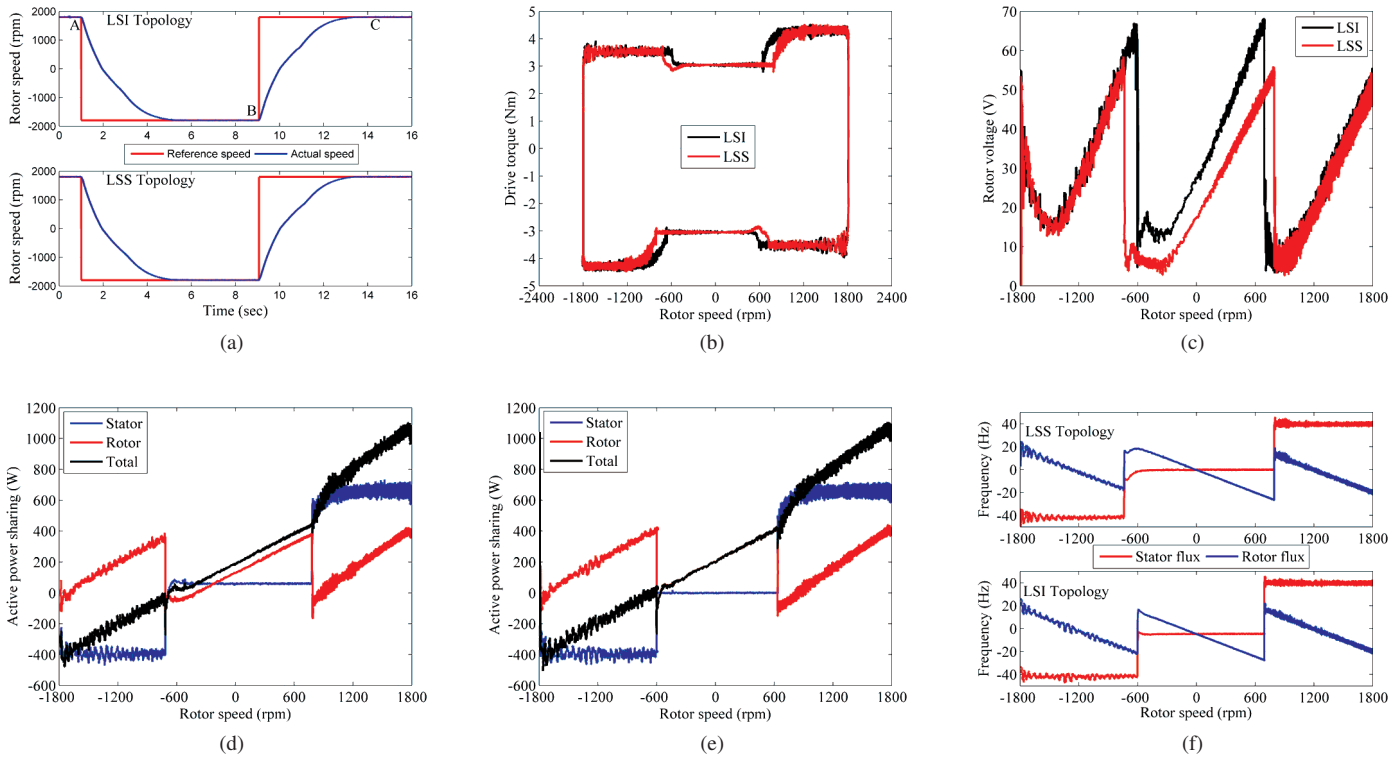

Figure 8. Experimental results to compare the two topologies for a full-speed range operation of the switched DFM drive. (a) Rotor speed (b) Drive torque (c) Required rotor voltage (d) Sharing of active power in LSS topology (e) Sharing of active power in LSI topology (f) Stator and rotor flux frequencies.

designed to be 775 rpm for the LSS topology and 615 rpm for the LSI topology each with a hysteresis band of ± 18 rpm. The dc electronic load bank is programmed to achieve a quadratic load torque profile with respect to shaft speed.

With the DFM initially running at 1800 rpm, a step-command in reference speed of -1800 rpm (at A in Fig. 8(a)) and back to 1800 rpm (at B) is given to the rotor speed controller. The speed performance of both the topologies are identical because of an equal drive torque capability. The estimated drive torque during this full-speed range operation is compared in Fig. 8(b). The only difference in the achieved drive torque is due to the difference in the mode transition speeds, each being optimized for the the individual topologies. Figure. 8(c) compares the required rotor voltages in the two topologies during the operation of the DFM with the positive drive torque (from B to C in Fig. 8(a)). For the example DFM, the required rotor voltage in the LSI topology is 18% higher compare to the LSS topology as expected due to higher operating stator flux level. The sharing of active power between the stator and rotor of the DFM in the two topologies are shown in Fig. 8(d) and 8(e) respectively. A power of 60 W is provided by the separate dc source to supply the losses in the stator winding during low-speed operation in the LSS topology. The maximum power supplied by the rotor power electronics is 5% higher in the LSI topology as compare to the LSS topology that accounts for the losses in the stator of the DFM. Finally, Fig. 8(f) shows the stator and rotor flux frequencies during the full speed range operation. The stator flux frequency in the LSS configuration is zero while in the LSI configuration is -5 Hz for positive drive torque for the example DFM.

IV. Conclusions

This paper compared two topologies of the switched DFM drive under different steady-state considerations. The comparison can be used not only to down-select the preferable topology for a given DFM design and specific drive requirements based on end-application but also to specify design guidelines for the DFM for a particular switched-DFM topology. Relative sharing of the magnetizing current to the DFM dictates the preferable choice of topology to achieve the torque capability of the DFM and minimize the required electrical power processing capability. Although the LSI topology has lower component counts, the LSS topology can have lower structural noises and vibration. In either topologies, the switched DFM drives has unique potential of reducing the required power converter size while operating over wide speed range with bipolar torque capability and will be suitable for many high power applications.

Acknowledgment

This research was performed with support from the Kuwait Foundation for the Advancement of Sciences (KFAS) through

the Kuwait-MIT Center for Natural Resources and the Environment (CNRE), the Skoltech-MIT SDP Program, and The Grainger Foundation.

REFERENCES

[1] S. Kouro, J. Rodriguez, B. Wu, S. Bernet, and M. Perez, "Powering the future of industry: High-power adjustable speed drive topologies," *Industry Applications Magazine, IEEE*, vol. 18, no. 4, pp. 26–39, July 2012.

[2] L. Parsa and H. Toliyat, "Five-phase permanent magnet motor drives for ship propulsion applications," in *Electric Ship Technologies Symposium, 2005 IEEE*, July 2005, pp. 371–378.

[3] C. Lewis, "The advanced induction motor," in *Power Engineering Society Summer Meeting, 2002 IEEE*, vol. 1, July 2002, pp. 250–253 vol.1.

[4] S. Muller, M. Deicke, and R. De Doncker, "Doubly fed induction generator systems for wind turbines," *Industry Applications Magazine, IEEE*, vol. 8, no. 3, pp. 26–33, May 2002.

[5] A. Tessarolo, G. Zocco, and C. Tonello, "Design and testing of a 45-mw 100-hz quadruple-star synchronous motor for a liquefied natural gas turbo-compressor drive," *Industry Applications, IEEE Transactions on*, vol. 47, no. 3, pp. 1210–1219, May 2011.

[6] J. Sayago, T. Bruckner, and S. Bernet, "How to select the system voltage of mv drives - a comparison of semiconductor expenses," *Industrial Electronics, IEEE Transactions on*, vol. 55, no. 9, pp. 3381–3390, Sept 2008.

[7] J. Rodriguez, S. Bernet, B. Wu, J. Pontt, and S. Kouro, "Multilevel voltage-source-converter topologies for industrial medium-voltage drives," *Industrial Electronics, IEEE Transactions on*, vol. 54, no. 6, pp. 2930–2945, Dec 2007.

[8] J. Rodriguez, B. Wu, S. Bernet, N. Zargari, J. Rebolledo, J. Pontt, and P. Steimer, "Design and evaluation criteria for high power drives," in *Industry Applications Society Annual Meeting, 2008. IAS '08. IEEE*, Oct 2008, pp. 1–9.

[9] S. Bernet, "Recent developments of high power converters for industry and traction applications," *Power Electronics, IEEE Transactions on*, vol. 15, no. 6, pp. 1102–1117, Nov 2000.

[10] B. Wu, *High-Power Converters and AC Drives*. IEEE Press, March 2006.

[11] A. Banerjee, M. Tomovich, S. Leeb, and J. Kirtley, "Power converter sizing for a switched doubly fed machine propulsion drive," *Industry Applications, IEEE Transactions on*, vol. 51, no. 1, pp. 248–258, Jan 2015.

[12] L. Morel, H. Godfroid, A. Mirzaian, and J.-M. Kauffmann, "Double-fed induction machine: converter optimisation and field oriented control without position sensor," *Electric Power Applications, IEE Proceedings -*, vol. 145, no. 4, pp. 360–368, Jul 1998.

[13] S. B. Leeb, J. L. Kirtley, W. Wichakool, Z. Remscrim, C. N. Tidd, J. A. Goshorn, K. Thomas, R. W. Cox, and R. Chaney, "How much dc power is necessary?" *Naval Engineers Journal*, vol. 122, no. 2, pp. 79–92, 2010.

[14] A. Banerjee, M. Tomovich, S. Leeb, and J. Kirtley, "Control architecture for a switched doubly fed machine propulsion drive," *Industry Applications, IEEE Transactions on*, vol. 51, no. 2, pp. 1538–1550, March 2015.

[15] A. Banerjee, A. Chang, K. Surakitbovorn, S. Leeb, and J. Kirtley, "Bumpless automatic transfer for a switched doubly-fed machine propulsion drive," *Industry Applications, IEEE Transactions on*, vol. PP, no. 99, pp. 1–1, 2015.

[16] G. Abad, J. López, M. Rodríguez, L. Marroyo, and G. Iwanski, *Doubly Fed Induction Machine: Modeling and Control for Wind Energy Generation*, ser. IEEE Press Series on Power Engineering. Wiley, 2011.

[17] I. Boldea, *Variable Speed Generators*, ser. Electric power engineering series. Taylor & Francis, 2006.

[18] J. Gieras, C. Wang, and J. Lai, *Noise of Polyphase Electric Motors*, ser. Electrical and Computer Engineering. CRC Press, 2005.

[19] D. Ross, *Mechanics of Underwater Noise*. Elsevier Science, 2013.

APPENDIX

Normalized steady-state d-axis and q-axis stator (v_{sd}, v_{sq}) and rotor voltage (v_{rd}, v_{rq}) equations:

$$v_{sd} = r_s i_{sd} \tag{8}$$

$$v_{sq} = \omega_s \psi_s + r_s i_{sq} \tag{9}$$

$$v_{rd} = r_r i_{rd} - (\omega_s - \omega_e)\psi_{rq} \tag{10}$$

$$v_{rq} = r_r i_{rq} + (\omega_s - \omega_e)\psi_{rd} \tag{11}$$

where r_s, r_r are the stator and rotor resistances and ω_s and ω_e are stator flux frequency and rotor shaft speed respectively.

Normalized flux equation for the stator (ψ_s) and rotor (ψ_{rd}, ψ_{rq}):

$$\psi_s = x_s i_{sd} + x_m i_{rd} \tag{12}$$

$$0 = x_s i_{sq} + x_m i_{rq} \tag{13}$$

$$\psi_{rd} = x_m i_{sd} + x_r i_{rd} \tag{14}$$

$$\psi_{rq} = x_m i_{sq} + x_r i_{rq} \tag{15}$$

where x_s, x_r, and x_m are the stator, rotor, and the mutual inductances respectively.

Electromagnetic torque equation:

$$\tau = -\frac{x_m}{x_s}\psi_s i_{rq} \tag{16}$$

For LSS topology:
At low speed,

$$v_{sd}^2 + v_{sq}^2 = v_{dc}^2;\ \omega_s = 0 \tag{17}$$

where v_{dc} is the dc-source voltage.
For LSI topology:
At low speed,

$$v_{sd} = v_{sq} = 0 \tag{18}$$

For both topology:
At high speed,

$$v_{sd}^2 + v_{sq}^2 = 1;\ \omega_s = 1 \tag{19}$$

Table I
EXAMPLE DFM PARAMETERS: 1 HP, 220-V/150-V, 4-POLE, 60-HZ, 3.6-A/4-A

Parameters	Actual	Normalized
Stator resistance	$3.575\ \Omega$	0.1013
Rotor resistance (ref. to stator)	$4.229\ \Omega$	0.1199
Stator leakage inductance	$9.6\ mH$	0.1024
Rotor leakage inductance (ref. to stator)	$9.6\ mH$	0.1024
Mutual inductance	$165\ mH$	1.763
Stator current rating	$5.09\ A$ (peak)	1
Rotor current rating (ref. to stator) (I_r)	$3.857\ A$ (peak)	0.7576